

Transient luminescence of dense InAs/GaAs quantum dot arrays

J. W. Tomm* and T. Elsaesser

Max-Born-Institut für Nichtlineare Optik und Kurzzeitspektroskopie, Max-Born-Strasse 2A, 12489 Berlin, Germany

Yu. I. Mazur

Department of Physics, University of Arkansas, Fayetteville, Arkansas 72701

H. Kissel

Ferdinand-Braun-Institut für Höchstfrequenztechnik, Albert-Einstein-Strasse 11, 12489 Berlin, Germany

G. G. Tarasov, Z. Ya. Zhuchenko, and W. T. Masselink

Department of Physics, Humboldt-Universität zu Berlin, Invalidenstrasse 110, 10115 Berlin, Germany

(Received 6 July 2001; revised 11 October 2002; published 31 January 2003)

Carrier transfer between quantum dots (QDs) in very dense InAs/GaAs QD arrays is studied by means of steady state and time-resolved photoluminescence spanning a wide range of laser power from 10^9 to 10^{13} photons/(pulse \times cm 2). Carrier transfer involves transitions from the ground state of small QDs into lower lying states of larger QDs, a relaxation channel that saturates at high excitation densities. The transition from saturation of the interdot carrier transfer to the unsaturated regime is identified by analyzing the temporal shape of the luminescence signal for decreasing excitation densities. The rate equation model is proposed to account the temporal evolution of photoluminescence in dense QD systems. Numerical simulations of the carrier transfer and relaxation including the interdot coupling are in good agreement with the experimental results.

DOI: 10.1103/PhysRevB.67.045326

PACS number(s): 78.55.Cr, 78.47.+p, 78.66.Fd

I. INTRODUCTION

Semiconductor quantum dots (QDs) are of high current interest, both for understanding the basic physics of quasi-zero-dimensional nanostructures and for applications. The properties of nonequilibrium electron-hole pairs localized in QDs are related to those of excitons being confined in spatial fluctuations of a low-dimensional, e.g., quasi-two-dimensional, confinement potential, a scenario which was studied extensively during the last decades.¹⁻³ A major difference between the two systems is the significantly wider spread of localization lengths and energies in semiconductor QD ensembles as well as the restricted number of available QD states. The latter property makes the QD system very interesting for studies of saturation effects in carrier transport and under optical excitation.

From the point of view of application, QDs may be useful for optoelectronic devices with improved parameters, such as reduced lasing thresholds, more robust surfaces, e.g., laser facets, etc. Ensembles with a high areal density D_a of QDs are required to achieve a sufficiently strong interaction between light and the device structure, e.g., in light-emitting or detecting devices. In such *dense QD arrays* with $D_a > 10^{10}$ cm $^{-2}$, the energy and carrier transfer between different QDs in the ensemble represent processes highly relevant for nonequilibrium carrier dynamics and—thus—affecting properties such as recombination, tunneling, carrier injection as well as lasing.⁴⁻⁷

Though there are numerous studies of the optical properties of QD arrays in the literature, carrier transfer processes in dense QD arrays are not understood in detail. The photoluminescence properties of dense arrays differ substantially from those of low-density ensembles, partly due to the dis-

tinctly different *bimodal* or even *multimodal* QD size distribution.⁸⁻¹¹ Time-resolved photoluminescence (PL) studies of dense QD arrays revealed mostly a monoexponential or biexponential decay of PL intensity on a time scale between several hundreds of picoseconds and several nanoseconds.¹²⁻¹⁴ This *exponential* behavior has been assigned to PL contributions from ground states of different QD sizes and/or to ground- and excited-state contributions. PL decay times τ_d derived from the observed exponential transients have been used to describe the dynamic behavior of the population $[n_i(t)]$ of the i th QD. This type of analysis, however, does not account for carrier transfer and coupling between different QDs which should result in finite risetimes of PL emission and/or a substantially modified decay behavior. Such issues have remained mainly unexplored. In this paper, we present a detailed investigation of carrier transfer in dense InAs/GaAs quantum-dot arrays. We demonstrate the occurrence of such transfer processes, strongly affecting the overall picosecond PL kinetics, in particular at very low excitation densities. A range of carrier densities in which interdot carrier transfer saturates is identified. This transfer involves transitions from higher-lying ground states of small QDs into lower-lying states of larger QDs.

The paper is organized as follows. Experimental techniques are described briefly in Sec. II. Experimental results for a wide range of excitation densities are presented and discussed in the main section (III). We introduce a conceptually simple model of picosecond carrier kinetics in dense arrays of coupled QDs taking into account radiative and non-radiative relaxation channels. Subsequently, a more sophisticated model is discussed which includes population saturation of the QD states and holds also for high excitation levels or small QD concentrations. Section IV contains some

conclusions, and is followed by an Appendix with the solution of rate equations.

II. EXPERIMENTAL DETAILS

A number of InAs/GaAs QD samples with different InAs layer thicknesses (d_{InAs}) were grown by gas-source molecular-beam epitaxy on semi-insulating (001) GaAs substrates. The samples consist of ten periods of 60-Å $\text{Al}_{0.2}\text{Ga}_{0.8}\text{As}$, 30-Å GaAs, 60-Å GaAs:Si ($N_D = 2 \times 10^{18} \text{ cm}^{-3}$), 60-Å GaAs, 4-Å to 7-Å InAs, 60-Å GaAs, 60-Å GaAs:Si, 30-Å GaAs, and 60-Å $\text{Al}_{0.2}\text{Ga}_{0.8}\text{As}$, subsequently capped with a 50-Å GaAs:Si layer. There are samples with and without Si doping in the superlattice. The dot containing layers are sufficiently separated that no significant vertical correlation is expected.¹⁵ The growth conditions (growth temperature T_G , d_{InAs}) are chosen to obtain high-density QDs.¹⁶ No systematic difference in the steady-state PL spectra was found for doped and undoped samples with the same InAs coverage.

Continuous wave (cw) steady-state PL was excited by the 514.5-nm line of an Ar^+ laser with excitation densities in the range from 1 mW/cm^2 to 20 W/cm^2 . Additional details concerning sample growth and characterization, particularly steady state PL, atomic force microscopy (AFM), and TEM, have already been reported elsewhere.¹⁶⁻¹⁹

Transient PL measurements were performed with sub-100-fs pulses from a Ti:sapphire laser ($\lambda = 732 \text{ nm}$, $\tau \approx 80 \text{ fs}$, $f = 82 \text{ MHz}$) allowing population of the InAs QDs by exciting the GaAs matrix. The PL emitted by the samples was spectrally dispersed in a 0.25-m monochromator and detected by a synchroscan streak camera equipped with an infrared enhanced S1 cathode. The overall time resolution of this detection system was 10 ps. The excitation density in the experiments was varied between 10^9 and 2×10^{13} photons/(pulse $\times\text{cm}^2$). Both steady-state and time-resolved luminescence experiments were performed at a sample temperature of 10 K.

III. EXPERIMENTAL RESULTS AND DISCUSSION

A. PL characterization of the quantum dot arrays

In the following, we mainly present experimental results for the sample that is representative for a larger number of similar structures having $d_{\text{InAs}} = 1.77 \pm 0.02 \text{ ML}$, which were separately grown under slightly different growth conditions. The dot sizes distribution derived from in-air AFM measurements (see details in Refs. 16 and 17) indicate the presence of two different QD families (or dot size modes), namely, one with an average base length $b = 8 \text{ nm}$ and a density of $D_a = 1.7 \times 10^{11} \text{ cm}^{-2}$, respectively, and another family with $b = 14.5 \text{ nm}$ and $D_a = 3 \times 10^{10} \text{ cm}^{-2}$, respectively.

The low-temperature steady-state PL spectrum of a sample with $d_{\text{InAs}} = 1.79 \text{ ML}$ is shown in Fig. 1. This broad PL band (the full width at half maximum is $\approx 120 \text{ meV}$) preserves its spectral shape when the excitation density is raised at least from 1 to 20 W/cm^2 . A line-shape analysis of the low-temperature spectrum shows that the PL signal is well reproduced by a convolution of two Gaussian-shaped

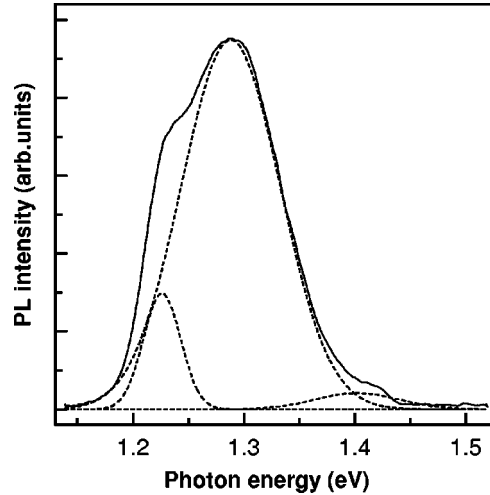


FIG. 1. Steady-state PL spectrum for a sample with $d_{\text{InAs}} = 1.79 \text{ ML}$ at $T = 10 \text{ K}$. A line-shape analysis of the low-temperature spectrum proves that the PL signal is a convolution of two Gaussian-shaped peaks and a third smaller contribution arising from the wetting layer.

peaks and a third contribution arising from the wetting layer (dotted lines in Fig. 1). Considering the size distribution and areal densities of both QD families, the stronger peak at 1.28 eV is attributed to the larger number of smaller QDs, having an average base length of 8 nm, while the lower-energy and weaker peak at 1.22 eV refers to larger dots with $b = 14 \text{ nm}$.

To support this assignment, we extended the intensity dependent PL measurements towards very high excitation densities. These measurements were done with pulsed excitation and the results are summarized in Fig. 2. For low excitation densities, a linear increase of the PL signal with excitation is found, similar to the cw PL measurements. The QD PL intensity at 1.22 and 1.28 eV begins to saturate at respective

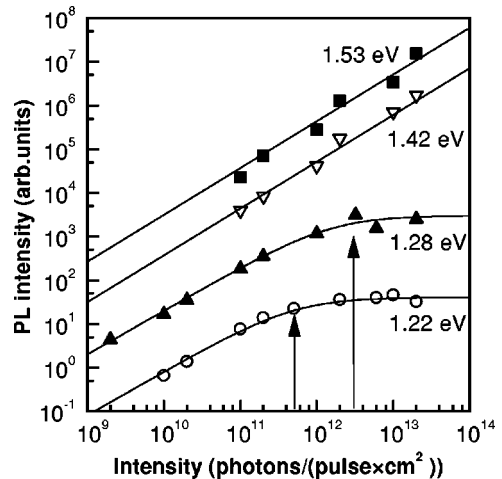


FIG. 2. PL signal magnitude vs excitation at $T = 10 \text{ K}$ measured in various spectral detection windows. The straight lines have the slope 1, and illustrate the linear PL response. For the QD luminescence, different saturation thresholds are found and marked by arrows.

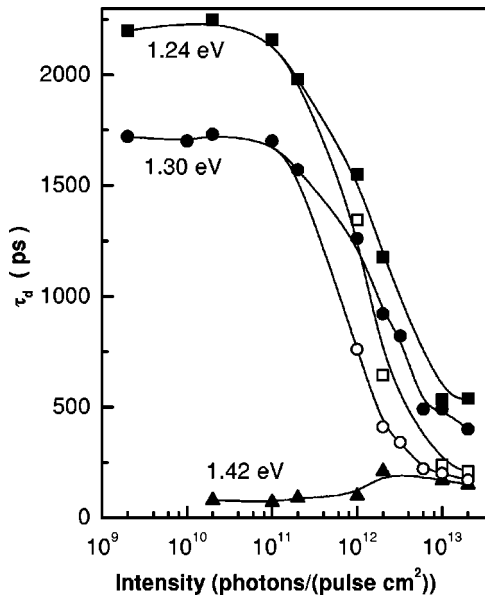


FIG. 3. PL decay time (τ_d) data determined from a least-square fit of transients for various excitation densities. The values are almost constant below 10^{11} photons/(pulse \times cm 2). Full symbols mark the long transients, whereas open symbols denote the faster transients that exclusively appear for high excitation densities.

excitation fluxes of about 5×10^{11} and 3×10^{12} photons/(pulse \times cm 2). The ratio of these “saturation fluxes,” about 1:6, again reflects the ratio of the D_a values for both QD families as determined by the AFM measurements. For the GaAs-matrix signal ($E=1.53$ eV) and the wetting layer luminescence ($E=1.42$ eV), linearity is maintained up to 2×10^{13} photons/(pulse \times cm 2). The absence of saturation for 1.42 and 1.53 eV, i.e., for wetting layer and GaAs matrix PL, gives additional confirmation that the saturation is caused by the limited number of available QD states.

B. Time-resolved photoluminescence

Time-resolved PL measurements were performed for different detection energies within the broad PL spectrum (Fig. 1) and in a wide range of excitation intensities. Up to excitation densities of 10^{11} photons/(pulse \times cm 2), the PL emission at the different detection energies rises within the time resolution of our experiment of 10 ps and displays a *monoexponential* decay characterized by a decay time τ_d . In Fig. 3, τ_d data determined from a least-square fit of the transients are summarized for different excitation densities. The values are almost constant below 10^{11} photons/(pulse \times cm 2). For higher excitation densities [$> 10^{11}$ photons/(pulse \times cm 2)] τ_d decreases, nonexponential transients appear, and finally a well-pronounced biexponential decay is observed at least in the spectral region of the QD emission band. In Fig. 3, the largest time constant measured, i.e. the one that is most likely to be governed by ground-state recombination, is marked by full symbols, whereas open symbols of the same type denote the additional faster components measured at the same photon energy for high excitation densities.

It is clearly seen from comparison of Figs. 2 and 3 that the magnitude of the PL signal saturates by two distinctly different saturation fluxes at the spectral positions of maximums of two Gaussian-shaped peaks (see Fig. 2), while the threshold for the appearance of biexponential decay is the same for both spectral positions (see Fig. 3). This latter fact can be ascribed to the intradot relaxation with the participation of excited QD states. However, the presence of faster components in the PL decay related to the excited states does not give evidence of the phonobottleneck existence in our dense QD system, while excited states do not develop at the elevation of cw excitation.

Besides switching from monoexponential to biexponential decay at higher excitation densities, a strikingly strong decrease of the PL decay time for the QD states is observed at higher excitation densities. Such a behavior is quite unusual in self-assembled QD systems. Indeed, the saturation effects expected under an elevation of the excitation density tend to produce longer carrier decay times in view of the exclusion principle. However, it can be wrong in a system of strongly coupled QDs with a large range of base lengths. In this latter case, the excited states of large QDs can be energetically close to the ground states of the small QDs. While the wave functions of the excited states are weakly localized in comparison with the ground state’s wave functions, the overlap of excited- and ground-state’s wave functions for neighboring QDs is stronger than the ground state’s wave-function overlap. In this case, the saturated states of large QDs can relax through the ground states of smaller QDs. The carriers will escape from large QDs into states with smaller relaxation time (smaller QDs), thus providing an effective reduction of the decay time through a complementary channel. This channel of energy relaxation can be of importance just for high-density QD systems.

C. Time-resolved photoluminescence for low excitation densities

We now present the interesting results measured at very low excitation densities which give evidence of a finite rise time of the PL at low detection energies, i.e., for large QDs. In Fig. 4(a), we plot the PL time evolution at a detection energy of 1.20 eV for excitation fluxes between 10^9 and 2×10^{11} photons/(pulse \times cm 2). For the lowest excitation densities, the PL signal was integrated over about 10^{11} subsequent excitation pulses. The data at low excitation clearly display a maximum shifted to positive times, a behavior which is indicative of a delayed rise to PL. With increasing excitation density, i.e., saturation of the QD ensemble, this maximum shifts to shorter times. For the highest density of 2×10^{11} cm 2 , the signal rises within the time resolution of 10 ps. As a measure for the delayed rise, we analyzed the temporal position of the maximum PL in each transient by fitting the whole curve. Figure 4(b) shows this temporal shift of the PL maximum versus excitation density. The position of the PL transient peak for 2×10^{11} photons/(pulse \times cm 2) was set as $t=0$. The line in Fig. 4(b) corresponds to a saturation curve with $t=t_0/(1+I/I_0)$, with $t_0=300$ ps and $I_0=1 \times 10^{10}$ photons/(pulse \times cm 2).

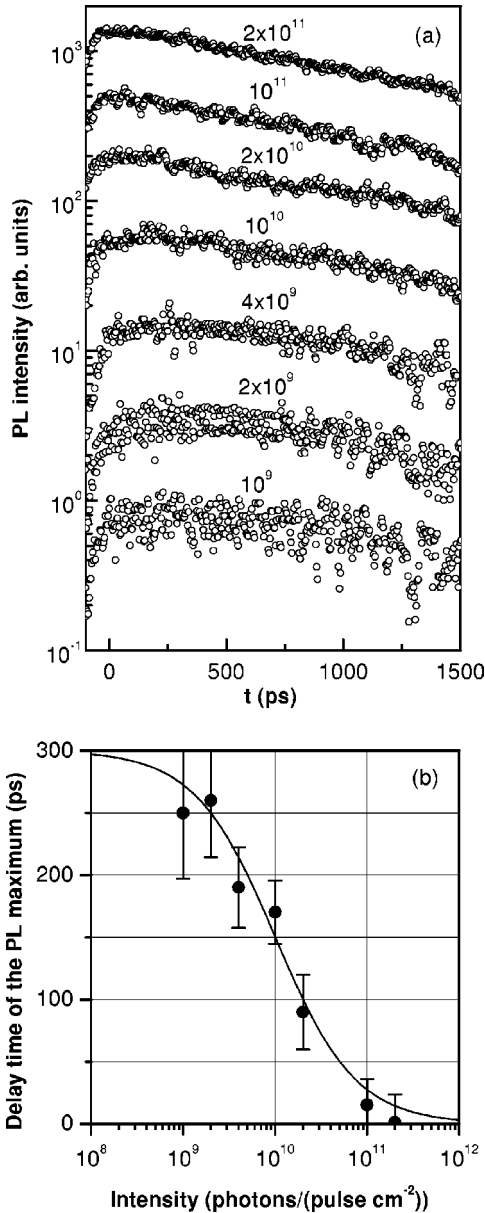


FIG. 4. (a) PL transients at 10 K for low and extremely low excitation densities. The detection energy is 1.2 eV. The intensity as parameter is given in photons/(pulse × cm²). (b) Shift of the PL maximum vs excitation density. The position of the PL transient peak for 2 × 10¹¹ photons/(pulse × cm²) was set to zero.

The delayed rise of PL for weak excitation is consistent with the model of interdot carrier transfer that considers the ground-state relaxation in a system of coupled QDs. In our model, carriers in the ground state of a QD can relax by radiative recombination giving rise to PL and—in addition—carriers populating the ground states of smaller QDs can be transferred into levels of larger QDs being even lower in energy.^{8,17} This represents an extra depopulation mechanism for the smaller sized dots and therefore the overall PL decay time τ_d becomes faster for smaller QDs, i.e., for increasing photon energy in the overall PL spectrum. Such a behavior was found in the experiments described above. Correspondingly, PL from large QDs exhibits different kinetics: First,

there is the population increase caused by accumulation of carriers that relax from smaller QDs, giving rise to a delayed rise of PL. Second, there is a decrease of the number of energy levels below the considered one into which the carriers might relax, resulting in longer PL decay times.

For weak excitation density of the QD ensemble and under the assumption that the carrier relaxation rate from an energy level in a QD is proportional to the number of vacant lower-energy levels in adjacent QDs, the rate equation for a particular quantum level E_i can be written as

$$\frac{dn_i}{dt} = -\frac{n_i}{\tau_0} - \sum_{j<i} \frac{n_i D_j}{\tau_i^{jj}} + \sum_{i<j} \frac{n_j D_i}{\tau_i^{ji}}, \quad (1)$$

where τ_0^i is the total ground-state recombination lifetime in the i th ground state, τ_i^{jj} is the interdot carrier transfer time between E_i and E_j states, and D_j is the density of the (final) E_j states. Equation (1) has an analytical solution given in the Appendix that allows a straightforward analysis of $n_i(t)$. The PL decay time τ_d is now calculated according to

$$\tau_d = -n_i(t) \frac{1}{\frac{dn_i(t)}{dt}}. \quad (2)$$

In fact, the proposed rate equations model of Eq. (1) holds for a dense QD system independent of the number of modes of its size distribution. The presence of more than one distinct dot size distribution within a large QD ensemble^{16,20,21} can be taken into account simply by introducing additional Gaussians into Eq. (1), resulting in several steplike variations of τ_d with emission energy.¹⁸ As a result, we find a staircaselike spectral dependence of ground-state luminescence time constants τ_d described in details in Ref. 18.

A realistic description of carrier dynamics in dense QD arrays has to include the case of saturation, i.e., situations in which the number of nonequilibrium carriers n_i reaches the number of available QD ground states N_j in the j th dot distribution. In order to include saturation effects, Eq. (1) is to be modified to

$$\frac{dn_i}{dt} = -\frac{n_i}{\tau_0} - \sum_{j<i} \frac{n_i(N_j - n_j)D_j}{\tau_i^{jj}} + \sum_{i<j} \frac{n_j(N_i - n_i)D_i}{\tau_i^{ji}}. \quad (3)$$

The equations of system (3) are nonlinear differential equations, and do not have an analytical solution. Therefore the system was solved numerically with the natural assumption of a single time τ_0 for the recombination lifetime in the i -th ground state and a single time τ_i for the interdot carrier transfer. The results are depicted in Fig. 5. The curves show the time evolution of PL from the QD system described in Sec. III A when $\gamma = \tau_i/\tau_0$ is equal 1. The transients are calculated at a photon energy of 1.22 eV, i.e., in the center of the lower-energy Gaussian, and different degrees of the ground states filling in the larger QDs. The “filling parameter”

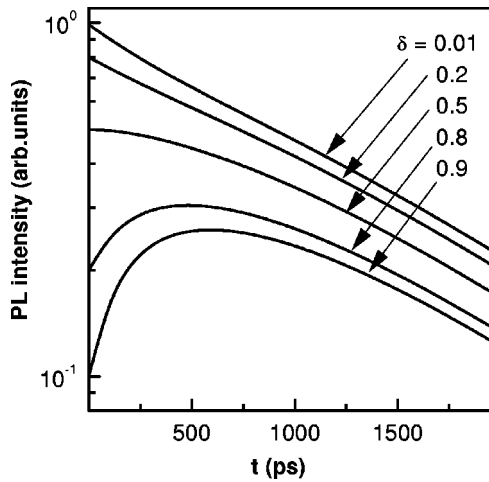


FIG. 5. Calculated PL transients for the QD system (Fig. 1) detected at 1.22 eV, i.e., in the center of the lower energy Gaussian, for different degrees of ground state filling in the larger QDs. $\gamma = \tau_r/\tau_0$ is a measure for the coupling, $\gamma=1$. The “filling parameter” δ gives the fraction of unoccupied QDs.

$$\delta = \frac{N_i - n_i}{N_i} \quad (4)$$

gives the fraction of unoccupied QDs and determines the initial conditions for the carrier relaxation in Eq. (3). The δ value is determined by the number of large QDs available in the dot size distribution, by the efficiency of carrier trapping into the QD’s ground state, and by the excitation density. Depending on these parameters, the δ value may vary within wide limits, from 1 for a completely unsaturated ground-state system to 0 for a saturated system.

The results displayed in Fig. 5 demonstrate a well-pronounced maximum of the PL transient for weakly filled QD ground states, e.g., at $\delta=0.9$, when the radiative recombination time (τ_0) and the carrier transfer time (τ_t) describing the interdot coupling are comparable, $\gamma \sim 1$. If the δ -value approaches 0 (the saturation case), the PL decay is again close to a single exponential. The exponentially decaying parts of the transients, e.g., the 1500–2000 ps range in Fig. 5, show a roughly constant slope resulting in about the same τ_d value independent of the initial ground-state filling. It is evident that saturation rather leads to exponential behavior, whereas the PL kinetics in the absence of saturation may also be described by the simpler model.

It should be noticed here that the only assumption in Eqs. (1) and (3) is the existence of lower- (upper-)lying states with respect to a certain state i in (from) which a carrier can appear (escape). Therefore, the model can also be applied to the temporal evolution of the PL in a system without interdot coupling, since the physical meaning of τ_t could be taken as an interdot transfer time as well as a nonradiative scattering time.

Applying this rate-equation model to the actual experimental situation, we can explain the details of QD kinetics. Indeed, transferring carriers from smaller to larger QDs results in a delayed buildup of population in the latter, a behavior reflected in the PL kinetics. With an increasing exci-

tation flux, saturation of the population in such low-energy states occurs, leading to a faster rise of PL. This experimental result is in full agreement with the predictions of the rate-equation models. For low excitation, we reach a regime where a simple model without saturation, i.e., a small filling factor δ , applies (Fig. 5). For strong excitation, saturation leads to a much faster population increase in the emitting QDs and a subsequent monoexponential decay of the PL intensity. Applying the simple model for the low-density case and using $t_0=300$ ps [Fig. 4(b)], we derive a value of $\gamma = \tau_t/\tau_0=1.3$. It is clear that the simple model seems not to be completely adequate to the real system by reason of the strong scattering of τ_0^i and τ_t^{ij} values that can be expected for the ground states of small-sized QDs. However, in high-density QD systems with a strong overlap of the wave functions and a great importance of QD size fluctuations as well as interdot distances, the individual characteristics of a single QD becomes substantially smeared, and an averaging over the relaxation times for both radiative recombination and carrier transfer in the QD ensemble becomes even of more physical meaning than those introduced for every isolated (or free-standing) QD. Taking a value $\tau_0 \sim 2.6$ ns corresponding to the PL decay time of the largest QDs where carrier transfer is almost absent, one finds an “averaged carrier transfer” time $\tau_t > 3.4$ ns for an individual transfer channel. Note that the much faster decay of PL from small QDs represents the sum over *all* possible transfer channels from such QDs into states at lower energies resulting in a short overall decay time.

A comment should be made on the mechanisms underlying interdot carrier transfer. For the strong quasi-zero-dimensional confinement in the InAs/GaAs system and the low sample temperatures in our experiments, activated transfer processes over barriers, e.g., by the absorption of optical phonons, can be ruled out. Our results might be interpreted in terms of multiphonon processes at low excitation densities and in terms of Auger processes at high excitation densities, as has been done for self-assembled InGaAs/GaAs (Ref. 22) and InAs/GaAs (Ref. 23) QDs. In case of Auger processes, the electron (hole) is assumed to be either immediately captured from the barrier into the QD ground state by transferring its energy to a second barrier electron (hole) or the electron is first captured into an excited QD state by an Auger process and relaxes down to the QD ground state afterward, gifting its energy partly to a barrier electron or even more probably to another electron inside the QD. Basically these processes have to be involved in the consideration in order to explain the carrier capture into a single QD and its ground-state population. They can be responsible for the value of the PL rise time, making it excitation density and wavelength dependent. In our model, the relaxation of the QD ground states is studied, and their populations serve already as the initial conditions for the set of equations (1). At this stage of relaxation (when the formation of rise time is completed), the Auger processes as well as the multiphonon processes become of low efficiency, and the interdot coupling including the quantum-mechanical coherency of the interacting state seems to be of great importance. Instead, lateral tunneling of carriers through barriers between adjacent QDs is con-

sidered as the main transfer mechanism.^{8,24} In Refs. 8 and 24, both lateral tunneling and tunneling between vertically stacked $\text{In}_{0.9}\text{Al}_{0.1}\text{As}$ (and InAs) QDs was discussed. For vertical tunneling with a well-defined barrier height of 140 meV and barrier thicknesses of 6, 8, and 10 nm, a good agreement between the measured tunneling times of 130, 370, and 850 ps and a semiclassical WKB description has been found. Applying a WKB model with similar barrier parameters to lateral tunneling, for our samples one estimates a tunneling time exceeding 100 ns, in striking contrast to our present experiments and the measurements reported in Ref. 8. There are several factors that might reduce the time constants for lateral tunneling. The lateral barrier height and width underlie strong statistical fluctuations, requiring an ensemble average to calculate the tunneling times. Furthermore, the presence of the InAs wetting layer with a continuum of electronic states may reduce the tunneling times. Even at low temperatures, tunneling assisted by acoustic phonons could enhance the overall transfer rates. In a very recent paper by Kalevich *et al.*,²⁵ the authors marginally reported on substantially decreased interdot transfer times in the case of weakly coupled dots by about four orders of magnitude in contrast to QD systems with still isolated dots ($D_a \leq 5 \times 10^{10} \text{ cm}^{-2}$). Since our experimental results prove interdot carrier transfer in our dense system ($D_a \sim 2 \times 10^{11} \text{ cm}^{-2}$) at low temperatures, a weak coupling with a decreased interdot transfer time is expected. This could also account for our as well as Tackuchi's (see Ref. 24) results and the observed deviation from the simple WKB approximation. A quantitative analysis of such mechanisms requires a fully quantum-mechanical description taking into account the QD size as well as the barrier width and height distribution in such systems. Such an analysis is beyond the scope of this experimental work.

An alternative explanation for a delayed rise of PL can be also derived from the analysis of Eqs. (1) and (3). From Eq. (1) it follows that a delayed rise of PL is obtained for $\gamma \approx 1$, when the nonradiative or carrier transfer time and the radiative time are comparable; the point is intuitive. Figure 5 further shows that, even for this situation, during saturation ($\delta \ll 1$) the PL decay again becomes monoexponential. It can be easily seen that at saturation power levels the last two nonlinear terms of Eq. (3) vanish, yielding the rate equation for monoexponential decay with a time constant close to τ_0 . Therefore, a delayed rise of PL can give evidence of some sort of bottleneck effect, that leads to longer transfer or relaxation times as compared with τ_0 . This seems to be an important result for relaxation dynamics in the case of dense QD systems. It is also clear that the decrease of τ_d at high pumping levels can arise from many-body effects, which become more important in a dense QD system due to the fact that carriers can readily scatter out of the saturated states. Within the empirical model this depopulation of the lowest-energy states could be treated by adding two similar nonlinear terms to rate equations (3) but with opposite signs and a different, shorter scattering time $\tau_d^*(P_{exc})$ (which is a function of laser power for high excitation). This would lead to an effective decrease in the PL decay time, as experimentally observed in the spectral range of the QD emission regardless

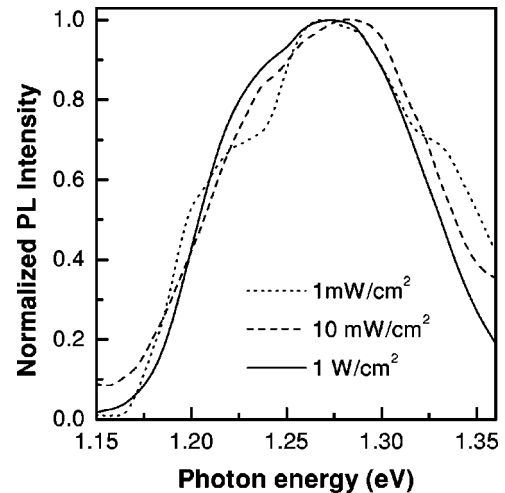


FIG. 6. Normalized cw PL spectra for the sample with $d_{\text{InAs}} = 1.79 \text{ ML}$ measured at low and extremely low excitation densities for $T = 10 \text{ K}$.

of QD size. This has little to do with the recombination times for higher-energy states (or of smaller dots) being shorter.

Finally, we conclude that a saturation of QD ground states takes place. In this case, however, one could expect a line-shape variation of the low-power cw PL on the basis of the saturation of the interdot carrier transfer mechanism. A thorough PL study at extremely low excitation densities (less than 1 W/cm^2) reveals such a modification. Figure 6 shows normalized cw PL spectra for excitation densities of 1 mW/cm^2 , 10 mW/cm^2 , and 1 W/cm^2 . It is clearly seen that increased excitation power leads to an enhanced low-energy part of PL spectrum, and a decay of the high-energy part. We find that the low-energy part reaches the saturation at 1 W/cm^2 . A further power increase does not change the line shape in this spectral region. The decay of the PL signal at the high-energy side of the PL band at very moderate excitation densities leads to a shrinking of the total PL spectrum. This effect can be assigned, e.g., to a carrier release from shallow traps within the wetting layer with subsequent transfer of them to the QDs when the pumping level increases. When the excitation density reaches 1 W/cm^2 no further change of the PL spectrum is observed.

IV. CONCLUSIONS

In summary, we reported a study of steady-state and transient photoluminescence of dense InAs/GaAs quantum dot arrays. Our data, taken at a sample temperature of 10 K, are consistent with the model of carrier transfer from small to large QDs within the ensemble directly influencing the PL kinetics. For low excitation densities, the low-energy states of large QDs display a delayed rise of PL due to the delayed accumulation of carriers transferred from smaller QDs. With an increasing excitation flux, the carrier population saturates, resulting in a fast rise of PL and a monoexponential decay. From a rate equation analysis of the time-resolved data, one derives a time constant of carrier transfer on the order of 3.5 ns. Interdot tunneling of carriers is considered the main

transfer mechanism at low temperatures. A theoretical model including the interdot coupling is proposed, and shows a qualitative agreement with our data. The behavior found here is highly relevant for the physics of dense arrays of coupled QDs.

ACKNOWLEDGMENT

The authors thank the Paul-Drude-Institut in Berlin for access to their AFM laboratory and especially A. Thamm for assistance. This work was supported by a DFG linkage grant.

APPENDIX

Equation (1) can be rewritten in more convenient form as

$$\frac{dn_i}{dt} = -\lambda_i n_i + \sum_{j=1}^{i-1} a_{ij} n_j. \quad (A1)$$

Here are

$$\lambda_i = \left(\frac{1}{\tau_0^i} + \sum_{j=i+1}^N \frac{D_j}{\tau_i^{ij}} \right) \quad \text{and} \quad a_{ij} = \frac{D_i}{\tau_i^{ji}}.$$

The index i labeling the levels runs from 1 for the one with the highest ground state energy, over all N states considered. The parameter λ_i determines the excitation decay into the state i and the corresponding a_{ij} value quantifies the energy transfer from higher energy states.

The solution of system (A1) satisfying the initial conditions $n_i = n_i^0$ can be written as follows:

$$n_i = \left(n_i^0 + \sum_{j=1}^{i-1} \varphi_{ij} \right) \exp\{-\lambda_i t\} - \sum_{j=1}^{i-1} \varphi_{ij} \exp(-\lambda_j t). \quad (A2)$$

The parameters of Eq. (A2) are calculated from the recurrent procedure,

$$\varphi_{11} = n_1^0,$$

$$\varphi_{ij} = \frac{a_{ji}}{(\lambda_j - \lambda_i)} \Theta_{ij} \varphi_{jj}, \quad i > j, \quad a_{11} = 0,$$

$$\Theta_{ij} = \begin{cases} 1 + \sum_{m=1}^{n=i-j-1} \left[(-1)^m \sum_{k=1}^{P_{mn}} \left\{ T(k,m) \prod_{l=1}^m A_l \right\} \right] & \text{if } i \geq j+2 \\ 1 & \text{if } i < j+2, \end{cases} \quad (A3)$$

$$A_l = \frac{a_{j\rho(k,l)}}{(\lambda_j - \lambda_{\rho(k,l)})} \frac{a_{\rho(k,l)r}}{a_{jr}},$$

$$\varphi_{ii} = n_i^0 + \sum_{k=1}^{i-1} \varphi_{ik},$$

$$P_{nm} = \frac{n!}{m!(n-m)!}.$$

Here P_{nm} is the number of combinations from n elements by m elements, $T(k,m)$ is the ordering operator that arranges all integer numbers $\rho(k,l)$ within the interval $j+1 \leq \rho(k,l) \leq i-1$ in descending order for every combination determined by the pair (k,m) in Eq. (A3), the index r is equal to i for $\max\{\rho(k,l)\}$ in any combination (k,m) and to the preceding value of $\rho(k,l)$ for every subsequent term in the ordered product (k,m) . Equation (A2) allows a straightforward analysis of $n_i(t)$. Nevertheless, it occurs not very informative in view of the huge number of input parameters τ_0^i and τ_i^{ij} typical for the ground states of a high-density QD system. In order to illustrate the characteristic features of QD kinet-

ics, it is therefore worthy to simplify the system assuming a single time τ_0 for the recombination lifetime in the i th ground state and a single time τ_i for the inter-dot carrier transfer. In what follows, we point out the physical reason for such a simplification even in the real case of high-density QD arrays. Under this assumption, Eq. (A3) includes the only modification

$$\Theta_{ij} = \begin{cases} \prod_{l=j+1}^{i-1} \left(1 - \frac{a_l}{\lambda_j - \lambda_l} \right) & \text{if } i \geq j+2 \\ 1 & \text{if } i < j+2, \end{cases} \quad (A4)$$

and it can be easily applied to the transient PL analysis. It should be noticed here that the only assumption in Eqs. (1) and (3) is the existence of lower (upper) lying states with respect to a certain state i in (from) which a carrier can appear (escape). Therefore, the model can be applied also to the temporal evolution of the PL in a system without interdot coupling since the physical meaning of τ_i could be taken as an interdot transfer time as well as a nonradiative scattering time.

*Electronic address: tomm@mbi-berlin.de

- ¹E. Cohen and M. Sturge, *Phys. Rev. B* **25**, 3828 (1982).
- ²C. Gourdon and P. Lavellard, *Phys. Status Solidi B* **153**, 641 (1989).
- ³S. Shevel, R. Fisher, E.O. Göbel, G. Noll, and P. Thomas, *J. Lumin.* **37**, 45 (1987).
- ⁴S. Sauvage, P. Boucaud, F.H. Julien, J.M. Gerard, and V. Thierry-Mieg, *Appl. Phys. Lett.* **71**, 2785 (1997).
- ⁵G. Yusa and H. Sasaki, *Appl. Phys. Lett.* **70**, 345 (1997).
- ⁶S. Fafard, *Appl. Phys. Lett.* **76**, 2707 (2000).
- ⁷R. Leon, S. Marcinkevičius, X.Z. Liao, J. Zou, D.J.H. Cockayne, and S. Fafard, *Phys. Rev. B* **60**, R8517 (1999).
- ⁸A. Tackeuchi, Y. Nakata, S. Muto, Y. Sugiyama, T. Usuki, Y. Nishikawa, N. Yokoyama, and O. Wada, *Jpn. J. Appl. Phys.* **34**, L1439 (1995).
- ⁹M. Paillard, X. Marie, E. Vanelle, T. Amand, V.K. Kalevich, A.R. Kovsh, A.E. Zhukov, and V.M. Ustinov, *Appl. Phys. Lett.* **76**, 76 (2000).
- ¹⁰H.D. Robinson and B.B. Goldberg, *Photonics Spectra* **6**, 444 (2000).
- ¹¹S. Marcinkevičius and R. Leon, *Appl. Phys. Lett.* **76**, 2406 (2000).
- ¹²S. Raymond, S. Fafard, P.J. Poole, A. Wojs, P. Hawrylak, S. Charbonneau, D. Leonard, R. Leon, P.M. Petroff, and J.L. Merz, *Phys. Rev. B* **54**, 11 548 (1996).
- ¹³R. Heitz, M. Veit, N.N. Ledentsov, A. Hoffmann, D. Bimberg, V.M. Ustinov, P.S. Kop'ev, and Zh.I. Alferov, *Phys. Rev. B* **56**, 10 435 (1997).
- ¹⁴R. Heitz, A. Kalburge, Q. Xie, M. Grundmann, P. Chen, A. Hoffmann, A. Madhukar, and D. Bimberg, *Phys. Rev. B* **57**, 9050 (1998).
- ¹⁵S. Fafard, Z.R. Wasilewski, C. Ni Allen, D. Picard, P.G. Piva, and J.P. McCaffrey, *Superlattices Microstruct.* **25**, 87 (1999).
- ¹⁶H. Kissel, U. Müller, C. Walther, W.T. Masselink, Yu.I. Mazur, G.G. Tarasov, and M.P. Lisitsa, *Phys. Rev. B* **62**, 7213 (2000).
- ¹⁷G.G. Tarasov, Yu.I. Mazur, Z.Ya. Zhuchenko, A. Maaßdorf, D. Nickel, J.W. Tomm, H. Kissel, C. Walther, and W.T. Masselink, *J. Appl. Phys.* **88**, 7162 (2000).
- ¹⁸Yu.I. Mazur, J.W. Tomm, V. Petrov, G.G. Tarasov, H. Kissel, C. Walther, Z.Ya. Zhuchenko, and W.T. Masselink, *Appl. Phys. Lett.* **78**, 3214 (2001).
- ¹⁹C. Walther, B. Herrmann, I. Hähnert, W. Neumann, and W.T. Masselink, *Superlattices Microstruct.* **25**, 53 (1999).
- ²⁰A.S. Bhatti, M. Grassi Alessi, M. Capizzi, P. Frigeri, and S. Franchi, *Phys. Rev. B* **60**, 2592 (1999).
- ²¹M. Grassi Alessi, M. Capizzi, A.S. Bhatti, A. Frova, F. Martelli, P. Frigeri, A. Bosacchi, and S. Franchi, *Phys. Rev. B* **59**, 7620 (1999).
- ²²B. Ohnesorge, M. Albrecht, J. Oshinowo, A. Forchel, and Y. Arakawa, *Phys. Rev. B* **54**, 11 532 (1996).
- ²³D. Morris, N. Perret, and S. Fafard, *Appl. Phys. Lett.* **75**, 3593 (1999).
- ²⁴A. Tackeuchi, T. Kuroda, K. Mase, Y. Nakata, and N. Yokoyama, *Phys. Rev. B* **62**, 1568 (2000).
- ²⁵V.K. Kalevich, M. Paillard, K.V. Kavokin, X. Marie, A.R. Kovsh, T. Amand, A.E. Zhukov, Yu.G. Musikhin, V.M. Ustinov, E. Vanelle, and B.P. Zakharchenya, *Phys. Rev. B* **64**, 045309 (2001).